

Operating Parabolic Troughs with Molten Salt: Solar Field Optimisation and Ternary Salt Properties

Dirk Krüger¹[\[https://orcid.org/0000-0002-8691-1141\]](https://orcid.org/0000-0002-8691-1141), Raphael Detzler²[\[https://orcid.org/0000-0001-9445-764X\]](https://orcid.org/0000-0001-9445-764X), Mark Schmitz²[\[https://orcid.org/0009-0003-7080-2260\]](https://orcid.org/0009-0003-7080-2260), Christian Jung¹[\[https://orcid.org/0000-0002-5893-4979\]](https://orcid.org/0000-0002-5893-4979), Alexander Bonk¹[\[https://orcid.org/0000-0002-0676-7267\]](https://orcid.org/0000-0002-0676-7267), Andrea Hanke¹[\[https://orcid.org/0000-0002-4137-7985\]](https://orcid.org/0000-0002-4137-7985), Pedro Horta³[\[https://orcid.org/0000-0002-7679-0200\]](https://orcid.org/0000-0002-7679-0200), Paula Martins³[\[https://orcid.org/0000-0003-1926-9993\]](https://orcid.org/0000-0003-1926-9993), Mehrdad Torabzadegan⁴[\[https://orcid.org/0000-0002-8777-4222\]](https://orcid.org/0000-0002-8777-4222), and Jana Stengler¹[\[https://orcid.org/0000-0001-6124-8286\]](https://orcid.org/0000-0001-6124-8286)

¹ German Aerospace Center (DLR), Germany

² TSK Flagsol Engineering GmbH, Germany

³ University of Évora, Portugal

⁴ Yara International ASA, Norway

Abstract. A variety of works have been performed at the Évora Molten Salt Platform on a new collector system especially designed for optimised operation with solar salt as well as tests on a ternary salt. Concerning the new HelioTrough[®] 3.1 design the paper discusses how 30% less specific mass could be reached. Together with a novel approach to “run-in” bearings, as to lower friction, the torsion could be reduced significantly. Resultingly costs were reduced while improving precision of the trough. The ternary salt has been operated between October 2021 and May 2022 in the end reaching operation temperatures up to 500°C. Samples have been taken and analysed to investigate nitrite and nitrate development amongst others. The heat capacity of the Yara Molten Salt has been determined with now a high level of precision, as well as the density.

Keywords: Parabolic Trough Collector, Ternary Salt, Yara Molten Salt, Solar Field Optimisation, HelioTrough[®] 2.0

1. Collector improvement

Certain lesson-learnt results associated with the use of molten salt as HTF in parabolic troughs in HPS-2 (HelioTrough[®] 2.0, “HT2”) have indicated that the collector design can be further improved [1]. Especially deformations (bending and torsion) of a continuous-beam torque tube structure as well as the alignment of the solar collector elements (SCE) of an SCA, have been identified as relevant to be minimized for an operation with molten salt because of the high concentration factors used. Accordingly, the reduction of bending and torsion has been targeted with the development from HT2 to the next generation collector, HT3. Also, a better method for collector alignment has been developed.

(1) Alignment

- a. Centering pin – in order to better align the SCE modules during field erection, a centering pin has been introduced at the frontend flange of SCE, allowing easy but centered turning of the modules against each other during mirror edge alignment.

(2) Bending and torsion

- a. SCE length – the HT2 torque tube with a length of 19 m showed relatively high bending, especially at the outermost SCE module of the collector. This has created low

points where substantial amounts of molten salt cannot be drained from. For HT3, a shorter system length of 17.86 m has been chosen for reduced module mass and bending.

- b. Torque tube design – the lugs of the torque tube, to which the (mirror bearing) cantilever arms are fixed, have now been designed as open ring stiffeners reducing tube buckling. Therewith a considerably lighter torque tube could be realized.
- c. Center of gravity – the weight of receiver posts could be reduced from 23.79 kg (HT2) to 16.54 kg and the mirror surface could be shifted towards the center of rotation by a change of mirror fixation and lug design, leading to smaller counterweights, less overall mass and subsequently lower bending (Figure 1).

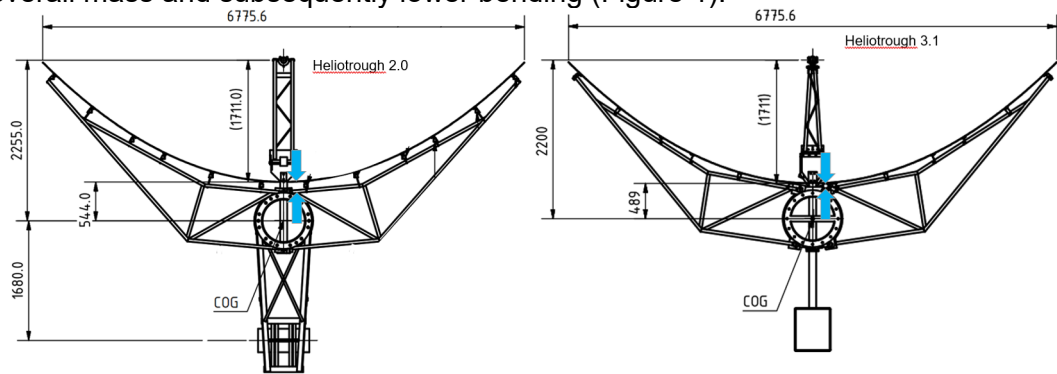


Figure 1. Geometries of HelioTrough[®] 2 (left) and 3 (right).

- d. Counterweights - the design and installation philosophy of counterweights has been changed from a 2-D adjustable design to a fixed one, facilitating the assembly process. The new connection to the torque tube reduces local stresses (Figure 2).

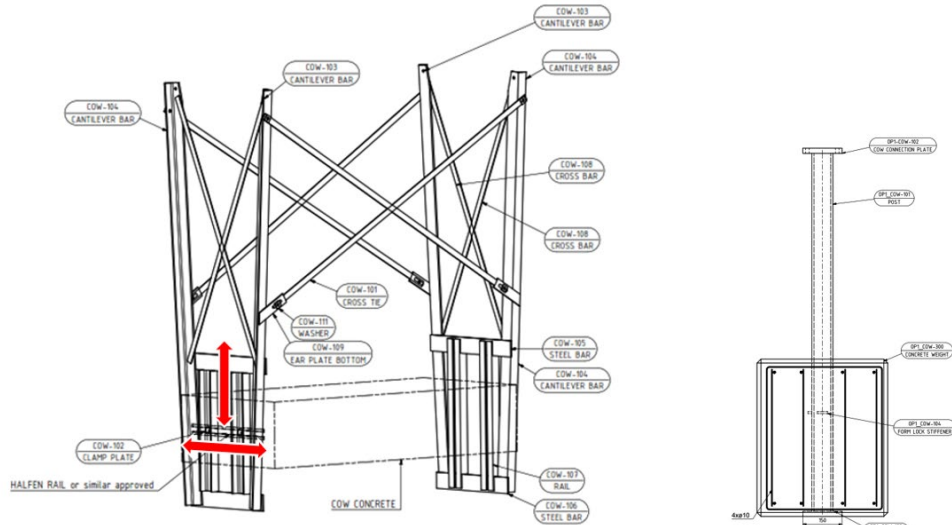


Figure 2. Design of counter weights of HelioTrough[®] 2 (left) and 3 (right).

- e. Moreover, the amount and position of the counterweights have been optimized in order to ensure minimal torsion at the collector end, as well as minimal local torsion at drive pylon, the latter improving focusing at higher inclination angles (Figure 3).

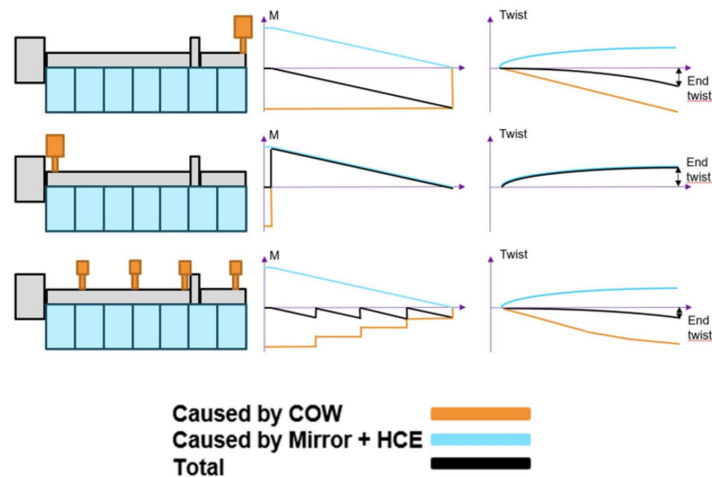


Figure 3. Torsional deflections by single and line loads.

- f. Support pattern – pylon distances were optimized for low bending and SCE flanges being vertical during installation, leading to a shorter distance between drive pylon and first middle pylon, as well as an overhanging SCE at the end of collector (Figure 4).

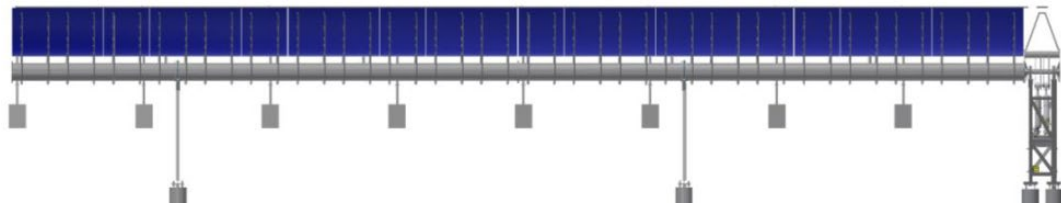


Figure 4. New support pattern of HelioTrough® 3.

- g. Bearing friction – the HT2 showed acceptable torsion at collector ends.

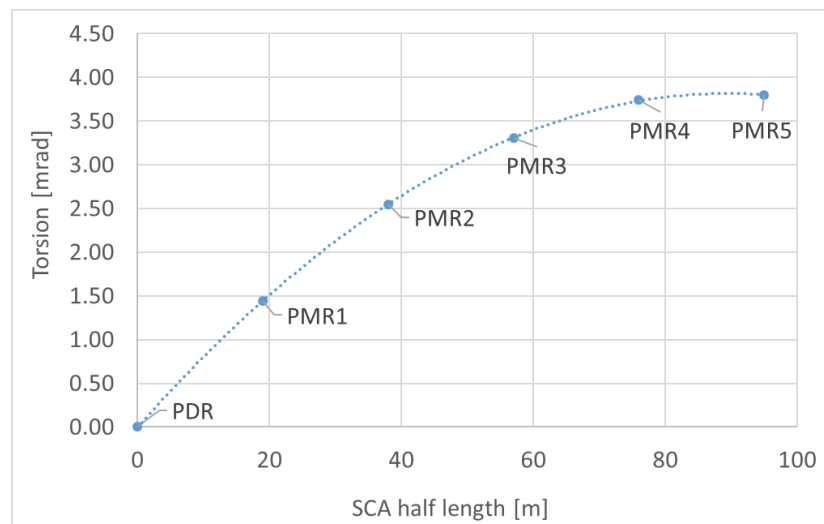


Figure 5. Torsion over collector length of HT2.0 - SCA3 (EMSP).

However, several effects, like increasing bearing friction over lifetime, can lead to far higher torsion and, thus, to tracking offset and performance loss (Figure 5).

Therefore, also the reduction of the initial friction of collector bearings has been investigated in order to reduce friction-induced torsion and bearing systems have been “run-in” with different parameters on a test bench, especially developed for this purpose within the project. The bearing test bench is installed at the EMSP (Figure 6).

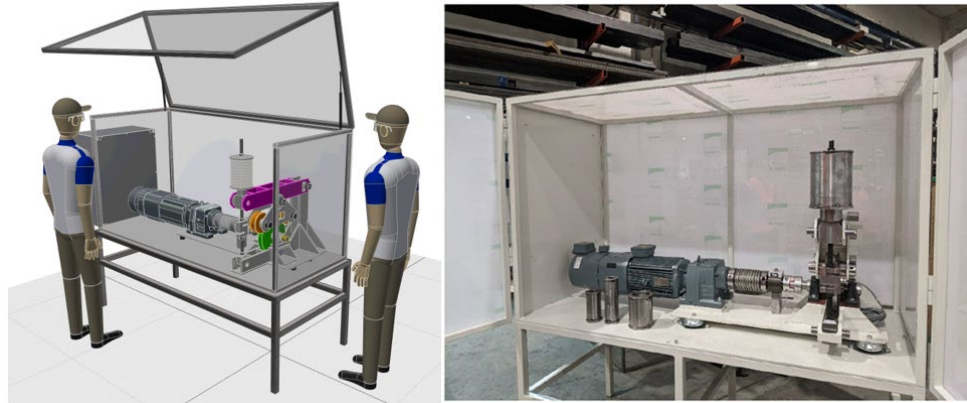


Figure 6. 3D model and photo of bearing test bench.

All effects together resulted in a reduction of specific mass by 30% while reducing dead-weight deflections by 70%. This also leads to better focusing at high inclination angles, aside from being far more cost effective in production. A torsion reduction can be reached by lower bearing friction, auto-balanced counterweights and centered alignment. All design changes were aimed at improved focusing because of higher concentration factors with molten salt application. The HelioTrough® Version 3.1 has been erected as a demonstrator on the EMSP (Figure 7).



Figure 7. 3D model and photo of HelioTrough® 3.1 demonstrator.

2. Testing physical data of ternary salt

For analysing the heat capacity of the unused Yara Molten salt mixture, a sample was prepared from 56.09 g NitCal-K (Yara), 38.06 g potassium nitrate (Haldor Topsoe) and 15.02 g sodium nitrate (BASF) in a 250 ml borosilicate lab bottle. After smelting at 180 °C for 23 hours mass loss was 8.31 g and increased after 24 hours at 200 °C to 8.57 g. Dried salt was transferred into a gold-plated stainless-steel crucible in oxygen atmosphere and heat capacity was determined in the closed crucible to avoid any mass losses which may be caused by creeping effects using a Calvet-type differential scanning calorimeter (sensys evo, Setaram). Correctness of the calibration of the DSC was checked with sapphire. Deviation to literature was less than 2% using the step method (10 K steps and 2 K/min heating rate). The unused Yara Molten Salt mixture was examined within 130 – 550 °C. Fig. 8 represents the average of two measurement runs of the same crucible up to 400 °C.

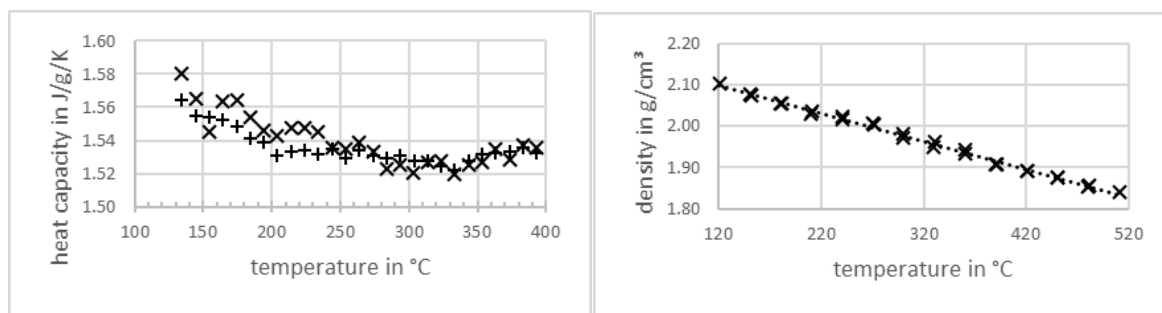


Figure 8. Physical properties findings of unused Yara Molten salt mixture; left: heat capacity using Calvet-type DSC and the step method; right: density via volumetric measurement.

Slightly decreasing values are found between 130 – 350 °C while steady increase is observed beyond 400 °C (not shown in Fig. 8). This increase beyond 400 °C is most likely caused by formation of nitrite which is currently investigated further. In a second measurement the crucibles were carefully filled with pure oxygen to suppress nitrite formation. Lower (apparent) increase of heat capacity is found due to this countermeasure. It is expected that heat capacity of the mixture remains more or less constant above 400 °C when the data are corrected with respect to nitrite formation.

For density measurement of the unused Yara Molten Salt mixture, a sample was prepared like described above. 17.09 g salt mixture were filled into a 10 ml measuring cylinder (high version, class A, DIN EN ISO 4788) which was placed inside a convection furnace equipped with calibrated Pt-100 sensor at the site of the sample. The filling level of the cylinder was recorded with an endoscopic camera system allowing volume measurements up to 600 °C. The volumes were recorded between 110 – 520 °C at thermal steps of 30 K within the heating up and cooling down phase. No significant sample loss occurred during the measurement. Gas formation was observed starting around 400 °C and getting more vigorous at higher temperatures indicating formation of oxygenation and nitrite. Nevertheless, strictly linear decrease of density was found (Fig. 8, right) indicating that no significant volume increase was caused by the amount of gas bubbles.

3. Post Analysis of Molten Salts after testing

During operation of the EMSF, about 50 molten salt samples were extracted mainly between January and May 2022 for analysis in DLR labs. Operation temperatures were slowly raised to finally 500 °C in the hot tank. Analysis was performed using wet-chemical methods from two labs simultaneously, and the data was consistent. The level of nitrates / nitrites and oxide ions which can form during thermal ageing of the molten salts, was analyzed and is plotted in Figure 9.

The levels of nitrate ions decrease while the levels of nitrite increase steadily over time until the end of the test campaign. The final levels of nitrate and nitrite ions are 98.8 mol% and 1.1 mol%, respectively, indicating that the nitrate ions partially decomposed according to the well-known nitrate-nitrite equilibrium reaction. Since the temperature of the tanks was steadily increasing over time, thermal equilibrium was not reached within the investigated time-frame. The levels of basic impurities originating from either CO₂ uptake (carbonate formation) or further decomposition (e.g. of nitrites into oxide ions) was also monitored. We observed varying findings of carbonate and oxide ion concentrations. The causes for these variations and the actual trend would need closer investigation over prolonged periods of testing. It is worth noting that during commissioning, precipitated residues were observed in the drainage tank (see Figure 11, right) which were found to consist of the original salt plus a large fraction of magnesium oxides and carbonates. They most likely originated from the decomposition of initially present

magnesium nitrate impurities and were not found to affect the system performance during operation.

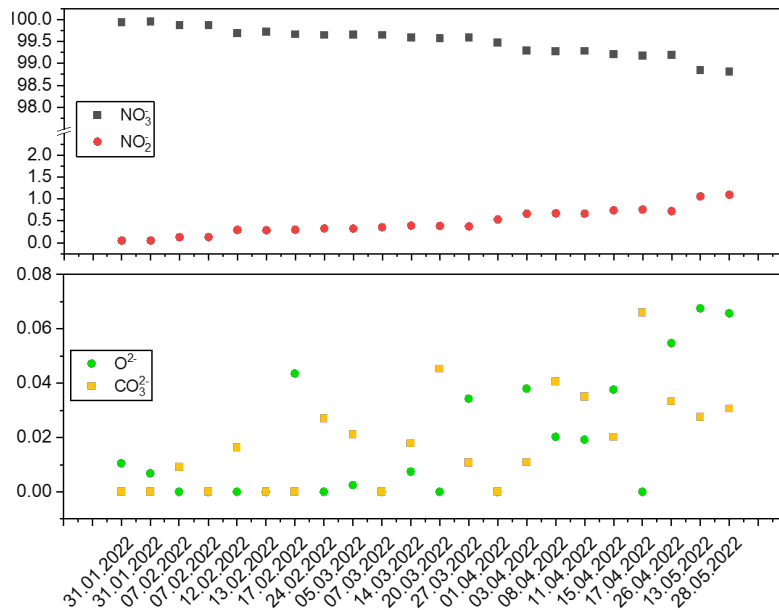


Figure 9. Top: Nitrate and nitrite levels in [mol%] in extracted salt samples during operation. Bottom: Carbonate and oxide-ion concentrations in [mol%] from the same samples.

A more detailed description of the operation can be found in [2].

4. Emptying the installation from salt

Experiences from filling solar fields with fluid salt and releasing it into tanks have been shared in publications as [3]. Descriptions and investigations of how to release fluent salt from tanks which have no release at the bottom or walls could not be found by the operating team or authors of this article. Therefore, this is described below in detail. In a first phase the HPS2 installation was operated with a ternary salt. Starting from beginning of June 2022 the salt has been removed from the solar field and tanks.

The hot salt has been pumped from one of the tanks onto a cooling belt (Figure 10, middle) which was connected with a flexible heated hose. The salt was frozen to pastilles with a diameter of around 3 mm and 2 mm in height and filled into big bags (Figure 10, left side). The infrastructure required for this was the installation of screw foundations, rental of a water chiller for cooling water supply, an oil heater for pre-heating, a flexible hose and a rented cooling belt. A total of about two weeks were required for commissioning of the cooling belt. Although pre-tests at the rental company of the belt went smoothly, the salt stuck to the belt. This was remedied by spraying a small amount of water and detergent on the belt. Critical was also the alignment of the belt and start-ups after changing the big bag. After gaining experience on optimal belt speed, salt mass flow and temperature, pastille size, cooling temperatures in commissioning it took around 100 hours to solidify and pack around 60 tonnes of the ternary salt.

However, the molten salt could not be completely removed, because the tanks are not equipped with releases. The long shaft immersion pumps have their suction nozzle in the height of approx. 500 mm above the bottom of the tanks.

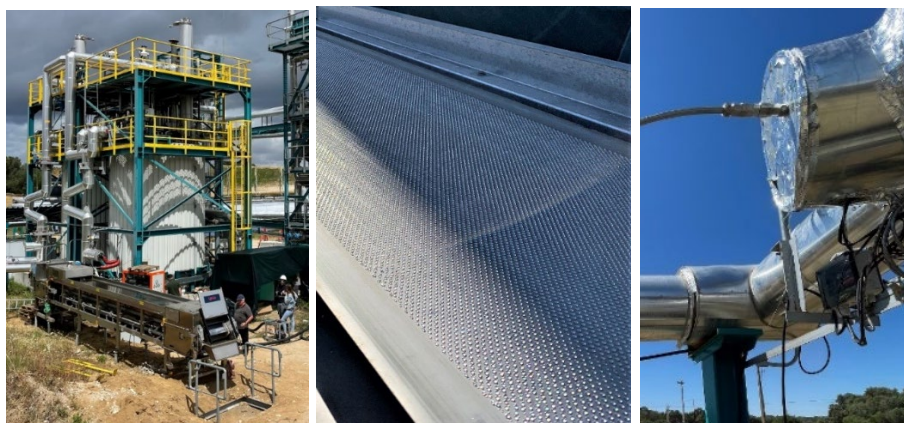


Figure 10. Left: Cooling belt, middle: Belt with salt prills on it, right: Trace heated injection point with full cone nozzle.

Therefore, a method was developed and studied in advance to dilute the salt with water so that it remains liquid at ambient temperature. Finally, an injection point was installed to the piping network with monitoring of the water mass flow and the pressure (Figure 10, right). 1 wt.% of water was injected into the salt with a temperature of 190°C and a pressure of 13 to 14 bar gauge pressure to avoid evaporation. It only took about 11 hours to decrease the salt temperature below 100°C by injecting around 13 m³ of demineralized water. This is much more than the required minimum water content of 4 wt.% to avoid fall out of solid salt crystal below 100°C. The process could go faster, but the operators were careful with the injection process. Then desalinated water was pumped directly into the tanks, because the water would not evaporate anymore at atmospherical pressure. No steam hammering or the like was audible, and the whole process proved to be unproblematic in other respects as well. The salt water could then be removed with simple sump pumps. About 30 tonnes of salt were diluted with 45 tonnes of water to come down below < 20°C with the clear point temperature.

After pumping all water/salt dilution out of the tanks an investigation of the tanks was possible, which is a seldom opportunity in large scale installations operated with salts. In the cold and the hot tank small amounts of solid calcium and magnesium compounds were found (Figure 11, left side). Larger amounts were found in the drainage tank (Figure 11, right side). Reasons are still under discussion. One reason might be that in this tank the cover was opened about 50 times between January and May for several minutes to first vent the tank before the personnel would take probes. Thus, CO₂ entered in the tank atmosphere. The other tanks were not opened. For all tanks CO₂ filters were installed at the air cooling inlet of the radar sensors. The air flow there was 20 liters/minute, that should have prevented air coming in at other points. The amount of CO₂ in the atmospheres of the tanks was not measured though. Calcium and Magnesium contents in e.g. solar salt may possibly lead to formation of solid components at high temperature operations. The solid material did not build up on the heatings although these were used. The material seems to have deposited more as a falling "dust", sinking on the ground. No baking on heating elements was found. Possibly the material deposited rather in areas with only minor salt flow velocities than other areas. These deposits did not influence the operation at the EMSP loop.

The dilution with water cannot simply be applied to solar salt. During the process the salt temperature must remain at a level so that it can be pumped and the pressure in the system must exceed the evaporation point of water to keep it fluent and avoid its immediate evaporation. For solar salt a safe pumping temperature would be about 290°C meaning a vapour pressure of roughly 80 bar for water. Typical solar salt installations are not equipped with a piping and instrumentation for this pressure level though. Thus for solar salt a release by valves at the bottom of the tank is crucial unless other methods can be found for emptying salt from tanks.



Figure 11. Left: Hot tank, right: Drainage tank.

Data availability statement

Data can be requested from the authors.

Author contributions

D. Krüger has mainly contributed to the chapter “Emptying the installation from salt”. Raphael Detzler and Dr. Mark Schmitz have contributed the chapter “Collector improvement”. Christian Jung has written about the physical properties of the salt. Alexander Bonk and Andrea Hanke analysed data for the chapter “Post Analysis of Molten Salts after testing”. Pedro Horta and Paula Martins were involved in funding acquisition and supervising the operation of the plant. Mehrdad Torabzadegan and Jana Stengler reviewed results.

Competing interests

The authors declare no competing interests.

Funding

The authors acknowledge the financial support by the German Federal Ministry for Economic Affairs and Climate Action. The sole responsibility for the contents lies with the authors.

References

1. Michael Wittmann, Mark Schmitz, and Hugo G. Silva, Peter Schmidt, and Günter Doppelbauer, and Ralph Ernst, and Patricia Santamaria, and Thorsten Miltkau, Dorin Golovca, Luís Pacheco, Daniel Högemann, Mirko Meyer-Grünefeldt, Bernhard Seubert. “HPS2 – Demonstration of Molten-Salt in Parabolic Trough Plants – Design of Plant”, SolarPACES 2018. <https://doi.org/10.1063/1.5117642>
2. Niklas C. Dicke, Mirko Meyer-Grünefeldt, Michael Wittmann, Jana Stengler, Pedro Horta, Paula Martins, Mehrdad Torabzadegan, Kai Schmitz, Mark Schmitz, Nils Gathmann, and Christian Stefan, “Demonstration of 3.5 MWth Parabolic Trough with Ternary Molten Salt at the Évora Molten Salt Platform”, SolarPACES Conference 2022 (submitted)
3. D. Kearney, B. Kelly, U. Herrmann, R. Cable, J. Pacheco, R. Mahoney, H. Price, D. Blake, P. Nava, N. Potrovitza, “Engineering aspects of a molten salt heat transfer fluid in a trough solar field”, *Energy* 29 (2004) 861–870, [https://doi.org/10.1016/S0360-5442\(03\)00191-9](https://doi.org/10.1016/S0360-5442(03)00191-9)